Scientific Inquiry and Review (SIR)
Volume 7 Issue 1, 2023
ISSN (P): 2521-2427, ISSN (E): 2521-2435
Homepage: https://journals.umt.edu.pk/index.php/SIR

Article QR

Title:	**Construction and Analysis of a Nonstandard Computational Method for the Solution of SEIR Epidemic Model**
Author (s):	Fazal Dayan, Muhammad Iqbal
Affiliation (s):	University of Management and Technology, Lahore, Pakistan
DOI:	https://doi.org/10.32350/sir.71.06
History:	Received: November 5, 2022, Revised: February 5, 2023, Accepted: February 6, 2023, Published: March 15, 2023
Citation:	Dayan F, Iqbal M. Construction and analysis of a nonstandard computational method for the solution of SEIR epidemic model. *Sci Inq Rev.* 2023;7(1):87–110. https://doi.org/10.32350/sir.71.06
Copyright:	© The Authors
Licensing:	This article is open access and is distributed under the terms of Creative Commons Attribution 4.0 International License
Conflict of Interest:	Author(s) declared no conflict of interest

A publication of
The School of Science
University of Management and Technology, Lahore, Pakistan

Construction and Analysis of a Nonstandard Computational Method for the Solution of SEIR Epidemic Model

Fazal Dayan * and Muhammad Iqbal

Department of Mathematics, School of Science, University of Management and Technology, Lahore, Pakistan

ABSTRACT

This paper is concerned with the numerical methods of susceptible exposed infectious recovered (SEIR) epidemic model of coronavirus disease 2019 (COVID-19). The model is explicated numerically with three numerical schemes, forward Euler, Runge-Kutta of order 4 (RK-4), and the proposed non-standard finite difference (NSFD) technique, respectively. In the epidemic model of infectious diseases, positivity is the main property of a consistent framework, since the negative value of a subpopulation is useless. The NSFD technique ends up being a more important and trustable numerical system than forward Euler and RK-4 techniques since it preserves positivity, stability, and convergence. On the contrary, forward Euler and RK-4 schemes do not hold these characteristics for some choices of step sizes. Numerical simulations confirmed the findings.

Keywords: convergence, NSFD method, SEIR model, stability

1. INTRODUCTION

In 1965, scientists identified the first human coronavirus case [1]. Later on, experts discovered a group of related human and animal illnesses caused by a family of viruses named coronaviruses after their crest-like appearance. People can contract seven types of coronavirus infections. COVID-19 sickness is a serious illness brought on by the SARS-CoV-2 infection [2]. The SARS-causing strain first appeared in southern China in 2002 and quickly spread to 29 different nations. By July 2003, 774 individuals had died and more than 8,000 had been infected [3]. Fever, headaches, and breathing problems, such as coughing and shortness of breath, are all brought on by coronavirus infection [4].

Middle East Respiratory Syndrome (MERS) first appeared in Saudi Arabia. Many people who were exposed to it developed difficulty in breathing. It was difficult to treat the respiratory illnesses of such people

* Corresponding Author: fazal.dayan@umt.edu.pk

and they could not recover without needing special care. People who have hidden illnesses, such as diabetes, cardiovascular disease, or risky development, are more likely to transfer recognized illnesses. Being educated about the condition and how the disease spreads is the greatest strategy to prevent and tone down its transmission.

On December 31, 2019, WHO received information regarding instances of pneumonia in Wuhan City, China with enigmatic explanations. On January 7, 2020, Chinese experts identified an original coronavirus as the cause and gave it the temporary designation '2019-nCoV' [5]. According to [6], USA and Brazil are the two nations that are most affected by COVID-19. Dhandapani et. Al provided stiff, fuzzy IRD-14 day average transmission model of COVID-19 pandemic disease [7]. To examine the factors involved in the spread of the coronavirus pandemic in Pakistan and its potential controls, S. Ullah and M.A. Khan developed a numerical model [8]. Duccio and Fanelli focused on the ephemeral aspects of the coronavirus disease 2019 in China, Italy, and France for the time period January 22 - March 15, 2020 [9]. The focus of Xiao and Ruan [10] remained on a pandemic model without a monotonic occurrence rate. The prescribed model depicts the psychological impact of specific illnesses on the local population as the number of infectious agents increase.

Since the spread of coronavirus has resulted in a pandemic, numerous mathematicians have conducted various analyses to create a model to predict its expansion [11–29].

The NSFD scheme was introduced by Mickens [23]. The construction of the NSFD mathematical model for a two-layered differential condition was the focus of Cresson and Pierret [24], who also investigated the model's various aspects, such as combination and solidness of the plan, among others. Selected mathematical models were established and tested using the RK method. Euler algorithm for requests 2 and 4 were completed. In order to account for a jungle fever model, Anguelov et al. [25] constructed the NSFD plot and investigated its dependability and constituent parts. To resolve the nonlinear Riccati differential condition, Riaz et al. [26] presented a very stable non-standard limited distinction (NSFD) strategy. By comparing the results to those of other mathematical operations, such as Euler and RK-4, the proposed model's accuracy and productivity were verified. A dynamic model for infection transmission components was proposed by Rafiq et al. [27].

A mathematical model is developed in the current study by comparing the results with prominent mathematical schemes including the Runge-Kutta approach and the Euler scheme. In order to investigate how insect vectors affect the development of plant diseases, Rafiq et al. [28] proposed a one-of-a-kind, genuinely stable, non-standard finite differentiation (NSFD) numerical arrangement. Numerical assessments were supplied and the outcomes were distinguished. In order to plan the proposed model and determine the value of the limit boundary R_0 for the model, Rafiq et al. [29] developed a model consisting of nonlinear differential conditions. To analyze the susceptible exposed infected recovered (SEIR) dynamic model of COVID-19 (coronavirus) with reference to bimodal infection transmission in vulnerable populations, Ahmed et al. [30] proposed a construction protecting nonstandard limited distinction plan. The suggested mathematical framework produced workable arrangements for the perplexing bi-modular SITR nonlinear model, combined actually consistent states, and reflected dynamic consistency with the perpetual feel of the model. The model's analysis revealed that it maintained some stability at focused consistent states. For the mathematical setup of the SEIR response dispersion pandemic model, [31] provided two innovative NSFD schemes. Moreover, [32] proposed an SIR model in a fuzzy environment. Euler, Runge Kutta of order 4 (RK-4, and the NSFD methods respectively were developed with fuzzy extensions for the solution of the model. Dayan et al. presented rumor based fuzzy model and developed an NSFD scheme for its solution [33]. Some researchers studied fuzzy epidemic models using NSFD schemes [34, 35]. Ali et al. applied the NSFD scheme for the numerical solution of a cancer disease model [36]. Alsallami et al. used Euler, RK, and NSFD methods to solve a real-world problem [37].

The remainder of this article is structured as follows. Model formulation is presented in Section 2. Section 3 discusses the model's equilibrium states, stability, and threshold analysis. Section 4 presents numerical simulation and discussion of the results, while Section 5 displays the numerical results. The novelty of the current work lies in the fact that the proposed model has not been analyzed before using the NSFD method.

2. SEIR MODEL FOR COVID-19

Consider the model

$$\frac{dS}{dt} = \Lambda - \mu S - \frac{\beta SI}{N} \quad (2.1)$$

$$\frac{dE}{dt} = \frac{\beta SI}{N} - (\mu + \epsilon)E \quad (2.2)$$

$$\frac{dI}{dt} = \epsilon E - (\gamma + \mu + \alpha)I \quad (2.3)$$

$$\frac{dR}{dt} = \gamma I - \mu R \quad (2.4)$$

2.1. Theorem

The system $(1-4)$ has a DFE point $(S_0, E_0, I_0, R_0) = (\frac{\Lambda}{\mu}, 0, 0, 0)$ and an endemic equilibrium point $(S^*, E^*, I^*, R^*) = \left(\frac{\Lambda}{\mu + \frac{\beta I}{N}}, \frac{\frac{\beta SI}{N}}{(\mu+\epsilon)}, \frac{\epsilon E}{\gamma+\mu+\alpha}, \frac{\gamma I}{\mu}\right)$, respectively.

2.2. Basic Reproductive Number

By incorporating the next generation matrix (NGM) approach, the value of R_0 is determined. Let $X = [S, E]^t$, then $\frac{dX}{dt} = y(x) - z(x)$, where

$$Y(x) = \begin{pmatrix} \frac{\beta SI}{N} \\ 0 \end{pmatrix}$$

and

$$Z(x) = \begin{pmatrix} (\mu + \epsilon)E \\ (+\gamma + \mu + \alpha)I - \epsilon E \end{pmatrix}.$$

Y and Z are now the Jacobeans of the $Y(x)$ and z(x) respectively at DFEP. They are listed below.

$$Y = \begin{pmatrix} 0 & \beta \frac{\beta \Lambda}{\mu N} \\ 0 & 0 \end{pmatrix}$$

and

$$Z = \begin{pmatrix} (\mu + \epsilon) & 0 \\ -\epsilon & \gamma + \mu + \alpha \end{pmatrix}.$$

Inverse of matrix Z is

$$Z^{-1} = \begin{pmatrix} \frac{1}{(\mu + \epsilon)} & 0 \\ \frac{\epsilon}{(\mu + \epsilon)(\gamma + \mu + \alpha)} & \frac{1}{(\gamma + \mu + \alpha)} \end{pmatrix}.$$

Computing the product $Y Z^{-1}$ we get,

$$YZ^{-1} = \begin{pmatrix} 0 & \beta \frac{\beta \wedge}{\mu N} \\ 0 & 0 \end{pmatrix} \begin{pmatrix} \frac{1}{(\mu + \epsilon)} & 0 \\ \frac{\epsilon}{(\mu + \epsilon)(\gamma + \mu + \alpha)} & \frac{1}{(\gamma + \mu + \alpha)} \end{pmatrix}$$

$$YZ^{-1} = \begin{pmatrix} \frac{\beta\epsilon}{(\mu + \epsilon)(\gamma+\mu+\alpha)} & \frac{\beta}{(\gamma+\mu+\alpha)} \\ 0 & 0 \end{pmatrix}.$$

Calculating the spectral radius of YZ^{-1} we get,

$$\lambda = \frac{\beta\epsilon}{(\mu + \epsilon)(\gamma + \mu + \alpha)}.$$

The spectral radius of YZ^{-1} is equable to R_0 which is the maximal eigenvalue of YZ^{-1}.

Therefore,

$$R_0 = \frac{\beta\epsilon}{(\mu + \epsilon)(\gamma + \mu + \alpha)}. \quad (2.5)$$

2.3. Normalized Forward Sensitivity Index (NFSI)

Chitins developed the idea of sensitivity indices by calculating the sensitivity indices of R_0 [38]. A parameter's normalized forward sensitivity index (NFSI) is calculated as $\text{NFSI}(\zeta) = \frac{\zeta}{R_o} \frac{\partial}{\partial \zeta}(R_0)$.

The NSFIs of β, ϵ, β, γ, and α are clalculated as follows:

$$\text{NFSI}(\beta) = \frac{\beta}{R_o} \frac{\partial R_0}{\partial \beta} = \frac{\beta}{\frac{\beta\epsilon}{(\mu+\epsilon)(\gamma+\mu+\alpha)}} \frac{\partial(\beta\epsilon)}{(\mu+\epsilon)(\gamma+\mu+\alpha)} = \frac{(\mu+\epsilon)(\gamma+\mu+\alpha)}{\epsilon} \frac{\epsilon}{(\mu+\epsilon)(\gamma+\mu+\alpha)} = 1.$$

Similarly,

$$\text{NFSI}(\epsilon) = \frac{\epsilon}{\frac{\beta\epsilon}{(\mu+\epsilon)(\gamma+\mu+\alpha)}} \frac{\partial\beta\epsilon}{\partial\epsilon(\mu+\epsilon)(\gamma+\mu+\alpha)} = \frac{\mu}{(\mu+\epsilon)}.$$

$$\text{NFSI}(\mu) = -\frac{\gamma}{(\mu+\epsilon)(\gamma+\mu+\alpha)}, \text{ and}$$

$$\text{NFSI}(\alpha) = \frac{\alpha}{(\gamma+\mu+\alpha)}.$$

These findings unambiguously demonstrate that β is the most sensitive parameter.

2.4. Stability Analysis

The Jacobean of the system (1-4) is

$$J = \begin{pmatrix} \mu - \beta\frac{I}{N} & 0 & -\beta\frac{S}{N} & 0 \\ \beta\frac{I}{N} & -(\mu+\epsilon) & \beta\frac{S}{N} & 0 \\ 0 & -\epsilon & -(\gamma+\mu+\alpha) & 0 \\ 0 & 0 & \gamma & -\mu \end{pmatrix}$$

$$J(\xi_0) = \begin{pmatrix} \mu & 0 & -\beta & 0 \\ \beta\frac{I}{N} & -(\mu+\epsilon) & \beta & 0 \\ 0 & -\epsilon & -(\gamma+\mu+\alpha) & 0 \\ 0 & 0 & \gamma & -\mu \end{pmatrix}$$

If the absolute eigenvalues of $J(\xi_0)$ are smaller than unity, that is, $|\lambda_i| < 1$, i = 1, 2, 3. The numerical scheme converges in all cases. The eigenvalue from the aforementioned Jacobean matrix were extracted, where $\lambda_1 = \lambda_4 = -\mu$, $\lambda_2 = -(\mu+\epsilon)$, and $\lambda_3 = -(\gamma+\mu+\alpha)$.

2.4.1. Stability at Endemic Equilibrium Point. Jacobean matrix at the EE point is

$$J(E^*) = \begin{pmatrix} \mu - \beta\frac{I^*}{N} & 0 & -\beta\frac{S^*}{N} & 0 \\ \beta\frac{I^*}{N} & -(\mu+\epsilon) & \beta\frac{S^*}{N} & 0 \\ 0 & -\epsilon & -(\gamma+\mu+\alpha) & 0 \\ 0 & 0 & \gamma & -\mu \end{pmatrix},$$

where

$S^* = \frac{\Lambda}{\mu+\beta\frac{I}{N}}$ and $I^* = \frac{\epsilon E}{(\gamma+\mu+\alpha)}$.

Using the MATLAB database, the biggest eigenvalues of $J(E^*)$ were plotted. At the endemic equilibrium point, the Jacobean spectral radius has a maximum value that is smaller than unity, as is evident from the preceding figure, proving the intended assertion.

3. NUMERICAL MODELING OF SEIR MODEL FOR COVID-19

3.1. Forward Euler Method

$$S^{n+1} = S^n + h[\Lambda - \mu S^n - S^n\frac{\beta I^n}{N}] \quad (3.1)$$

$$E^{n+1} = E^n + h\left[\frac{\beta S^n I^n}{N} - (\mu+\epsilon)E^n\right] \quad (3.2)$$

$$I^{n+1} = I^n + h\ [\epsilon E^n - (\gamma + \mu + \alpha)I^n\ ] \quad (3.3)$$

$$R^{n+1} = R^n + \mathrm{h}\ [\gamma I^n - \mu R^n] \quad (3.4)$$

3.2. Fourth Order Runge-Kutta (RK-4) Scheme

3.2.1. Step 1

$$k_1 = S^n + h[\Lambda - \mu S^n - S^n\frac{\beta I^n}{N}] \quad (3.5)$$

$$m_1 = E^n + h[\frac{\beta S^n I^n}{N} - (\mu+\epsilon)E^n] \quad (3.6)$$

$$n_1 = I^n + h\ [\epsilon E^n - (\gamma + \mu + \alpha)I^n\ ] \quad (3.7)$$

$$p_1 = R^n + \mathrm{h}\ [\gamma I^n - \mu R^n] \quad (3.8)$$

3.2.2. Step 2

$$k_2 = h[\Lambda - \mu(S^n + \frac{k_1}{2}) - \beta\frac{(S^n + \frac{k_1}{2})(I^n + \frac{n_1}{2})}{N}] \quad (3.9)$$

$$m_2 = h[\beta\frac{(S^n + \frac{k_1}{2})(I^n + \frac{n_1}{2})}{N} - (\mu+\epsilon)(E^n + \frac{m_1}{2})] \quad (3.10)$$

$$n_2 = h\ [\epsilon(E^n + \frac{m_1}{2}) - (\gamma + \mu + \alpha)(I^n + \frac{n_1}{2})] \quad (3.11)$$

$$p_2 = \mathrm{h}\ [\gamma(I^n + \frac{n_1}{2}) - \mu(R^n + \frac{p_1}{2})] \tag{3.12}$$

3.2.3. Step 3

$$k_3 = h[\Lambda - \mu(S^n + \frac{k_2}{2}) - \beta\frac{(S^n + \frac{k_2}{2})(I^n + \frac{n_2}{2})}{N}] \tag{3.13}$$

$$m_3 = h[\beta\frac{(S^n + \frac{k_2}{2})(I^n + \frac{n_2}{2})}{N} - (\mu + \epsilon)(E^n + \frac{m_2}{2})] \tag{3.14}$$

$$n_3 = h\ [\epsilon(E^n + \frac{m_2}{2}) - (\gamma + \mu + \alpha)(I^n + \frac{n_2}{2})] \tag{3.15}$$

$$p_3 = \mathrm{h}\ \left[\gamma\left(I^n + \frac{n_2}{2}\right) - \mu\left(R^n + \frac{p_2}{2}\right)\right] \tag{3.16}$$

3.2.4. Step 4

$$k_4 = h[\Lambda - \mu(S^n + k_3) - \beta\frac{(S^n + k_3)(I^n + n_3)}{N}] \tag{3.17}$$

$$m_4 = h[\beta\frac{(S^n + k_3)(I^n + n_3)}{N} - (\mu + \epsilon)(E^n + m_3)] \tag{3.18}$$

$$n_4 = h\ [\epsilon(E^n + m_3) - (\gamma + \mu + \alpha)(I^n + n_3)] \tag{3.19}$$

$$p_4 = \mathrm{h}\ [\gamma(I^n + n_3) - \mu(R^n + p_3)] \tag{3.20}$$

3.2.5. Step 5

$$S^{n+1} = S^n + \frac{1}{6}\ [k_1 + 2k_2 + 2k_3 + k_4\ ] \tag{3.21}$$

$$E^{n+1} = E^n + \frac{1}{6}\ [m_1 + 2m_2 + 2m_3 + m_4\ ] \tag{3.22}$$

$$I^{n+1} = I^n + \frac{1}{6}\ [n_1 + 2n_2 + 2n_3 + n_4] \tag{3.23}$$

$$R^{n+1} = R^n + \frac{1}{6}\ [p_1 + 2p_2 + 2p_3 + p_4] \tag{3.24}$$

3.3. Non-Standard Finite Difference (NSFD) Scheme

To develop an explicit NSFD scheme, consider the above system as

$$\frac{df(t)}{dS} = \frac{f(t+h) - f(t)}{h} + 0(h) \qquad h \to 0.$$

S^n, E^n, I^n, and R^n are approximations. Here, h is the time step size.

$$\frac{S^{n+1} - S^n}{h} = \Lambda - \mu S^{n+1} - S^{n+1}\frac{\beta I^n}{N} \quad (3.25)$$

$$S^{n+1} = \frac{S^n + h\Lambda}{1 + h\mu + h\frac{\beta I^n}{N}} \quad (3.26)$$

$$E^{n+1} = \frac{E^n + h\frac{\beta S^n I^n}{N}]}{1 + h(\mu + \epsilon)} \quad (3.27)$$

$$I^{n+1} = \frac{I^n + h\,\epsilon E^n}{1 + h\,(\gamma + \mu + \alpha)} \quad (3.28)$$

$$R^{n+1} = \frac{R^n + h\,\gamma I^n}{1 + h\mu} \quad (3.29)$$

3.4. Stability Analysis of the NSFD Technique

The NSFD scheme of the SEIR model is carried out in this section at DFEP $(S_0, E_0, I_0, R_0) = (\frac{\Lambda}{\mu}, 0, 0, 0)$. Consider the **Eq.** (**3.25**) to (**3.28**),

$$F = S^{n+1} = \frac{S + h\Lambda}{1 + h\mu + h\frac{\beta I}{N}} \quad (3.30)$$

$$G = E^{n+1} = \frac{E + h\frac{\beta SI}{N}]}{1 + h(\mu + \epsilon)} \quad (3.31)$$

$$H = I^{n+1} = \frac{I + h\,\epsilon E}{1 + h\,(\gamma + \mu + \alpha)} \quad (3.32)$$

$$K = R^{n+1} = \frac{R + h\,\gamma I}{1 + h\mu} \quad (3.33)$$

Jacobean matrix of the **Eq.** (**3.30**) to (**3.33**) at the DFEP is as follows:

$$J(\xi_0) = \begin{pmatrix} \frac{1}{1+h\mu} & 0 & -\frac{(\frac{\Lambda}{\mu}+h\Lambda)(\frac{h\beta}{N})}{[1+h\mu]^2} & 0 \\ 0 & \frac{1}{1+h(\mu+\epsilon)} & \frac{h\beta\Lambda}{\mu N} & 0 \\ 0 & \frac{h\epsilon}{1+h(\gamma+\mu+\alpha)} & \frac{1}{1+h(\gamma+\mu+\alpha)} & 0 \\ 0 & 0 & \frac{h\gamma}{1+h\mu} & \frac{1}{1+h\mu} \end{pmatrix}.$$

The eigenvalues of the aforementioned Jacobean matrix are $\lambda_1 = \frac{1}{1+h\mu} < 1$ and $\lambda_2 = \frac{1}{1+h\mu} < 1$. The following matrix is used to compute the remaining eigenvalues.

$$J(\xi_0) = \begin{pmatrix} \frac{1}{1+h(\mu+\epsilon)} & \frac{h\beta\Lambda}{\mu N} \\ \frac{h\epsilon}{1+h(\gamma+\mu+\alpha)} & \frac{1}{1+h(\gamma+\mu+\alpha)} \end{pmatrix}.$$

The other eigenvalues are quite complicated to be calculated algebraically. Therefore, they have been calculated numerically (shown in Figure 1).

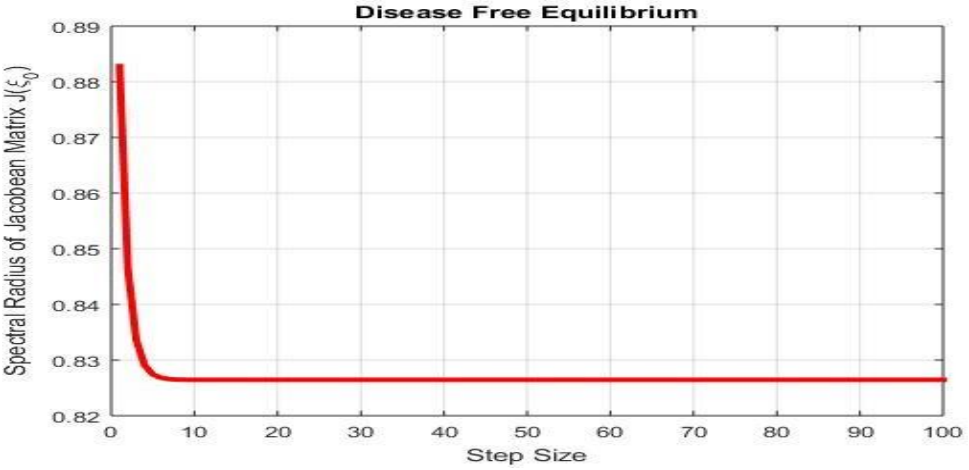

Figure 1. Eigenvalues of $J(\xi_0)$

The spectral radius of the Jacobean matrix at the DFE point has a maximum value that is less than unity, as is evident from the following figure, proving the intended assertion.

4. NUMERICAL SIMULATION OF THE SEIR MODEL

The findings are discussed in detail in this section. Additionally, Euler, RK-4, and NSFD methods in the model are compared in terms of their use.

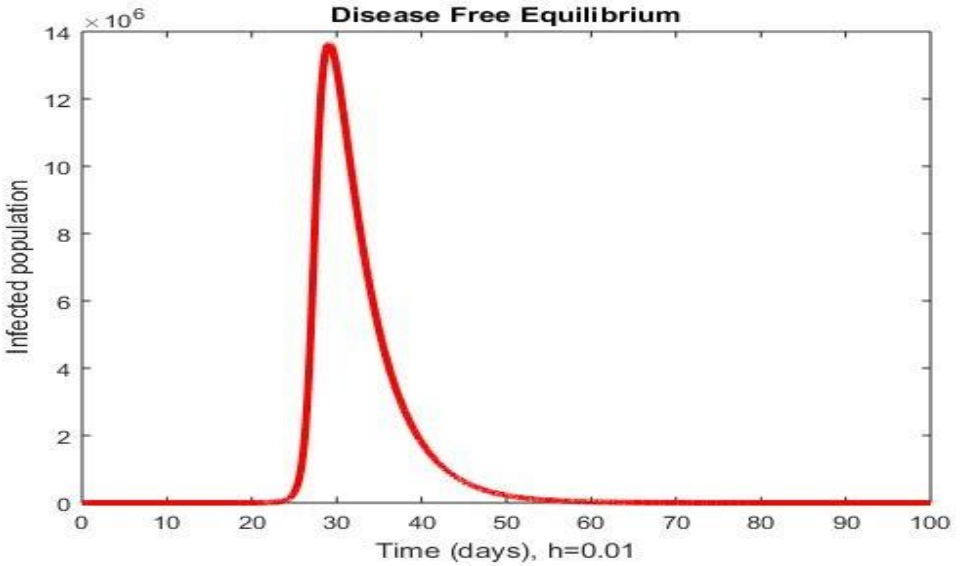

Figure 2. Infected Population using Forward Euler Scheme at h =0.0

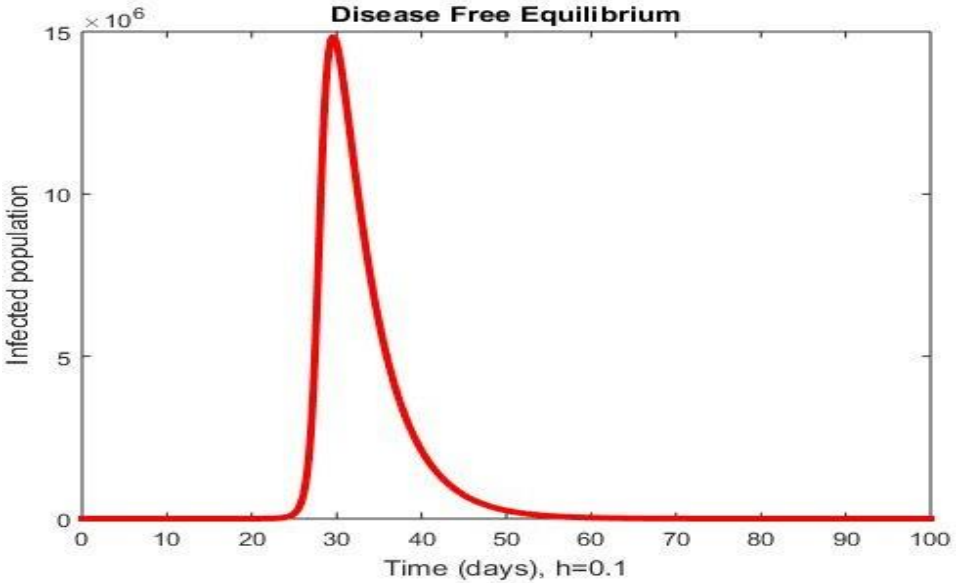

Figure 3. Infected Population using Euler Scheme at h =0.1

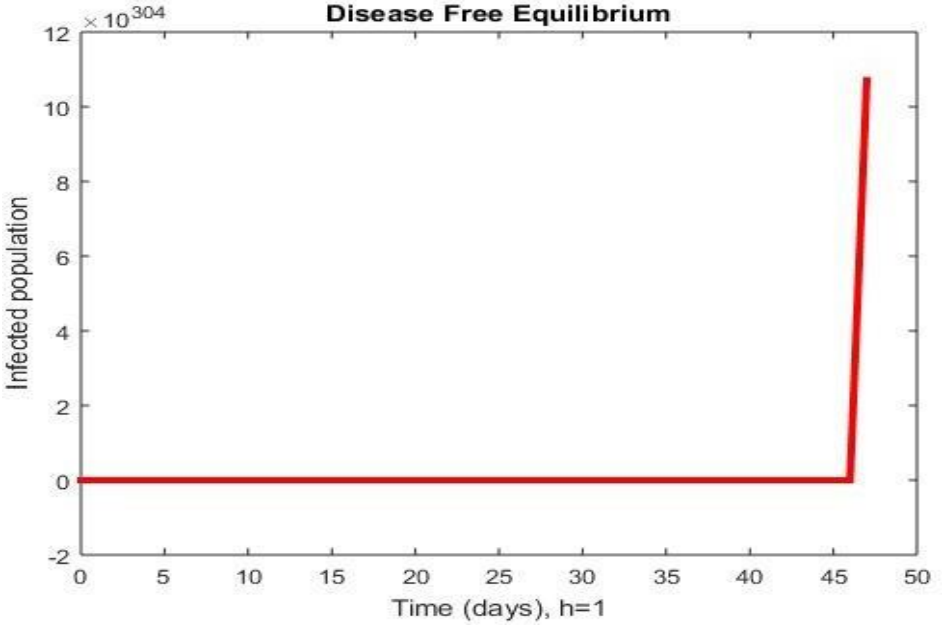

Figure 4. Infected Population using Euler Scheme at h =1

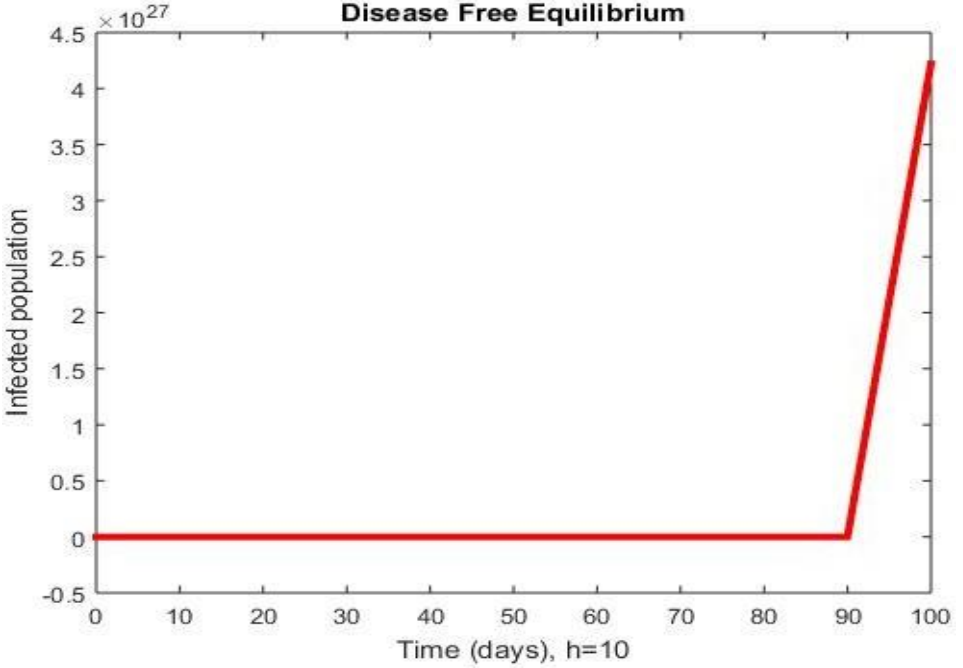

Figure 5. Infected Population using Euler Scheme at h =10

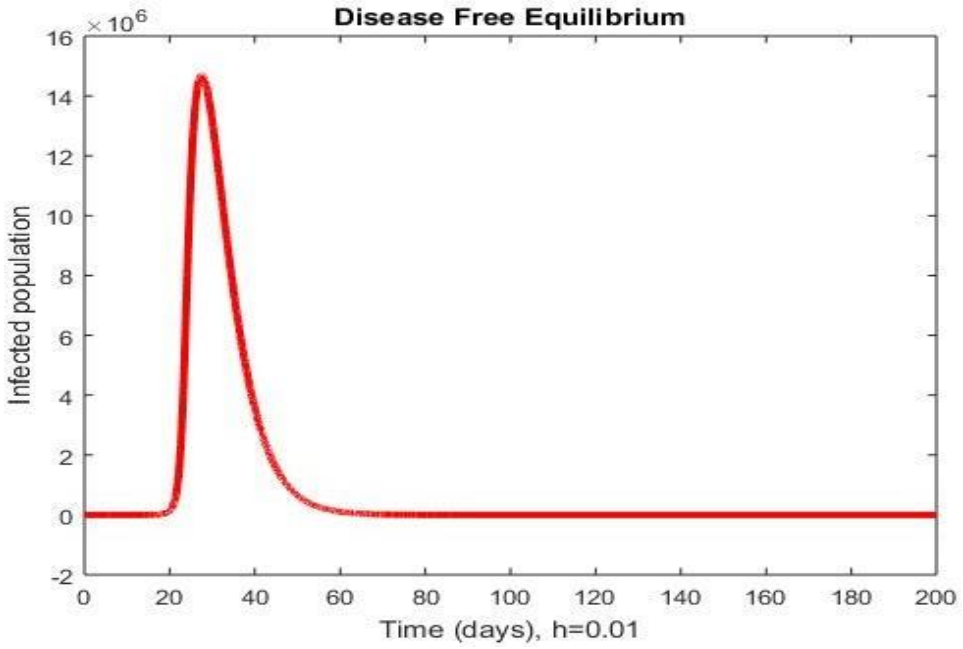

Figure 6. Infected Population using RK-4 Method at h =0.01

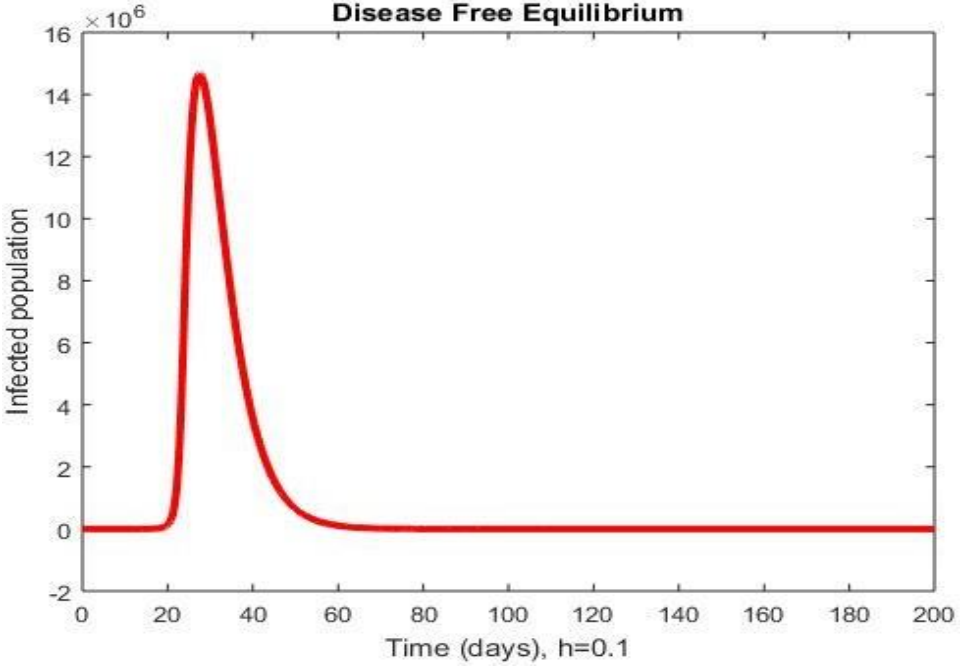

Figure 7. Infected Population using RK-4 Method at h =0.1

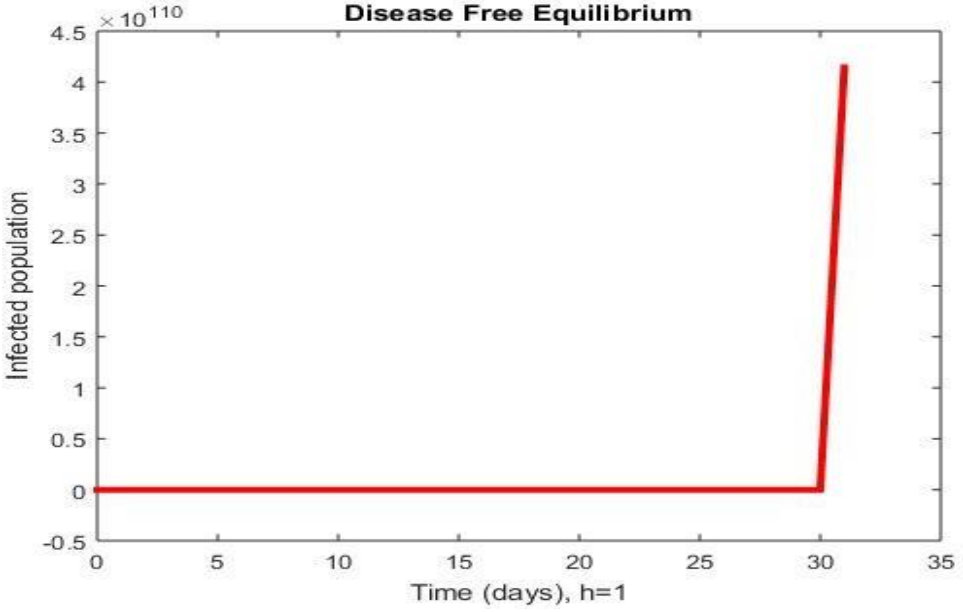

Figure 8. Infected Population using RK-4 Method at h =1

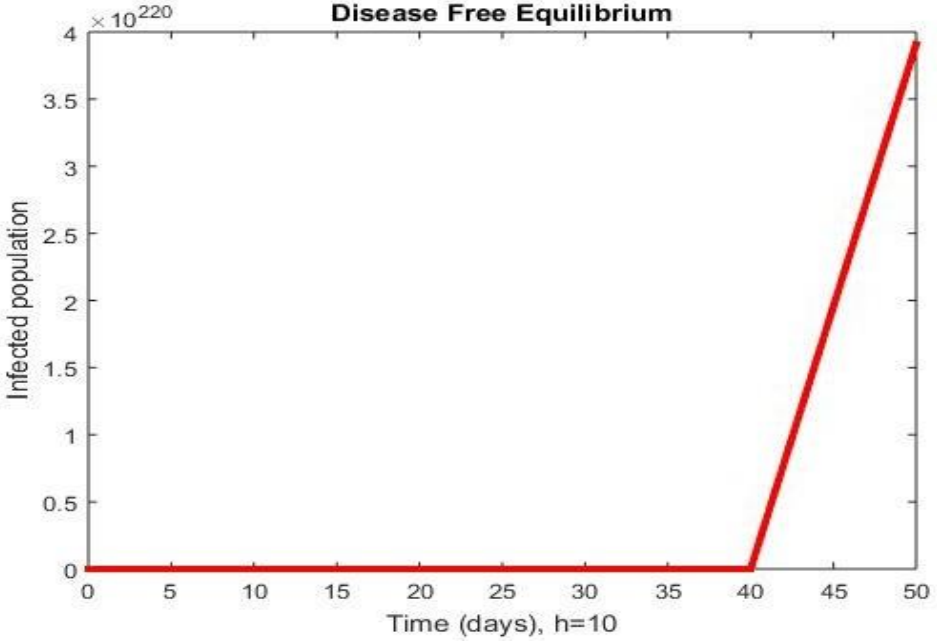

Figure 9. Infected Population using RK-4 Method at h =10

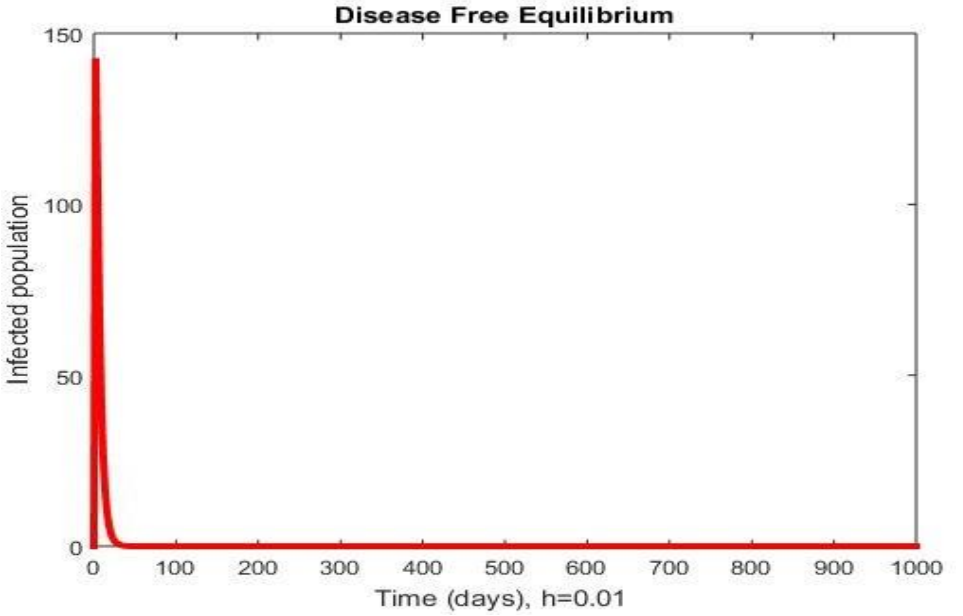

Figure 10. Infected Population using NSFD Scheme at h =0.01

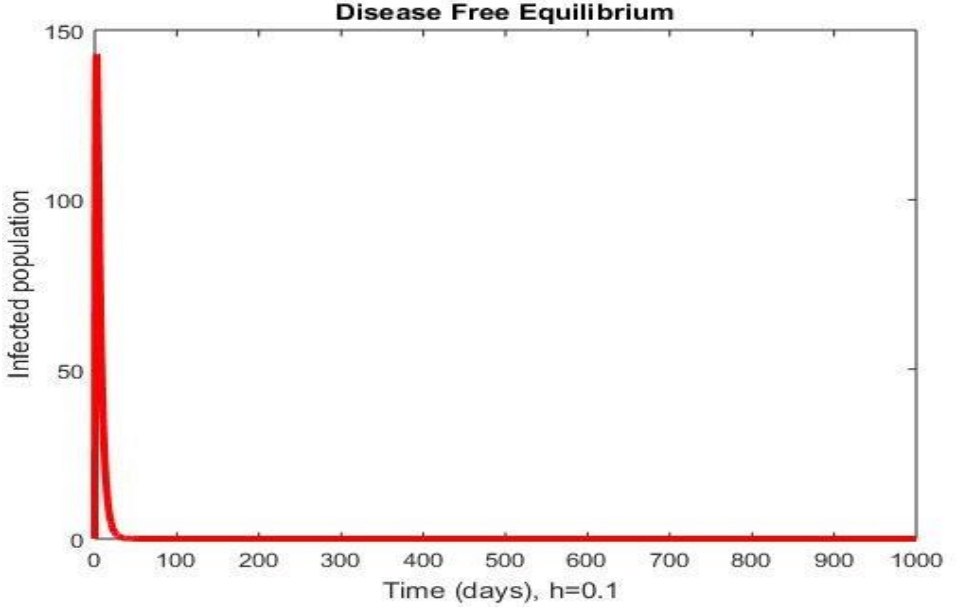

Figure 11. Infected Population using NSFD Scheme at h =0.1

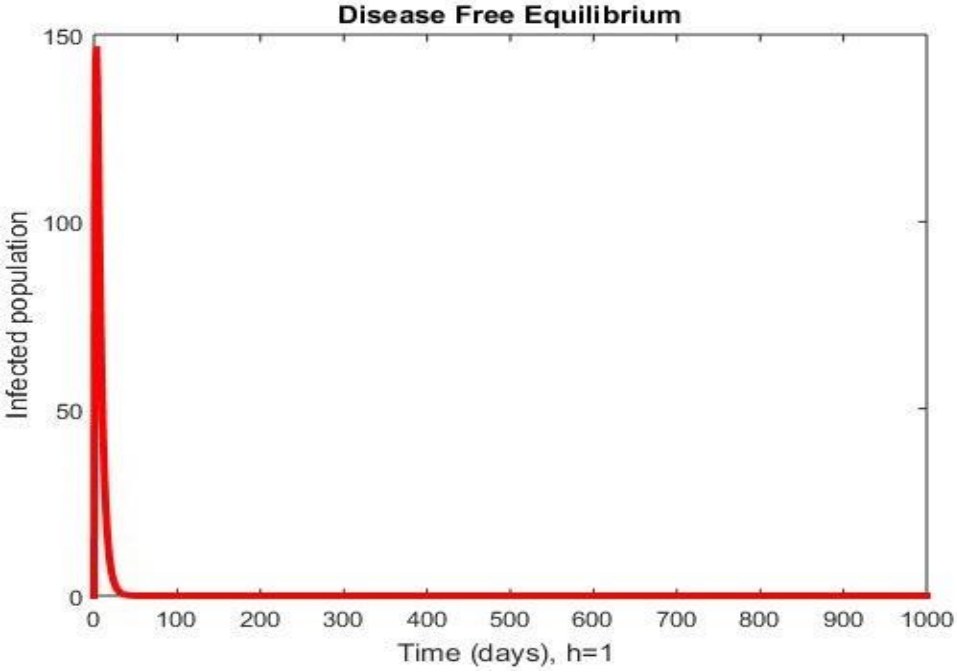

Figure 12. Infected Population using NSFD Scheme at h =1

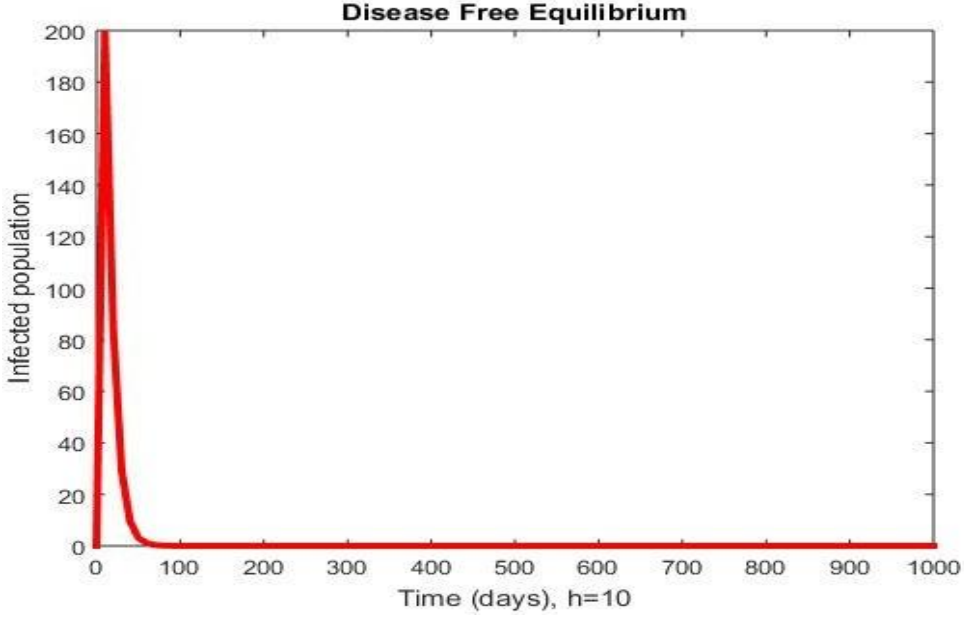

Figure 13. Infected Population using NSFD Scheme at h =10

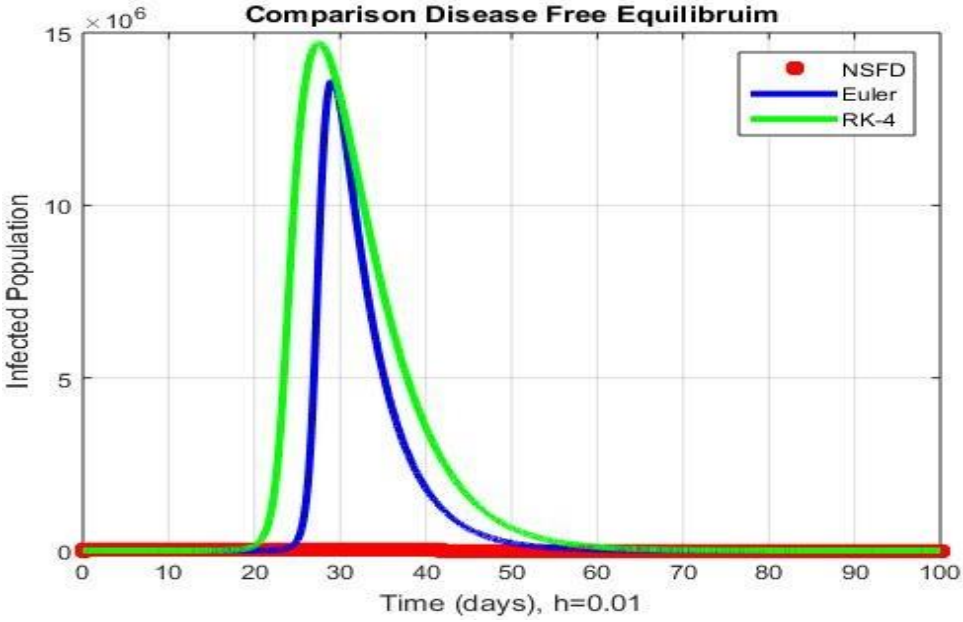

Figure 14. Comparison of Euler, RK-4, and NSFD Scheme at h=0.01

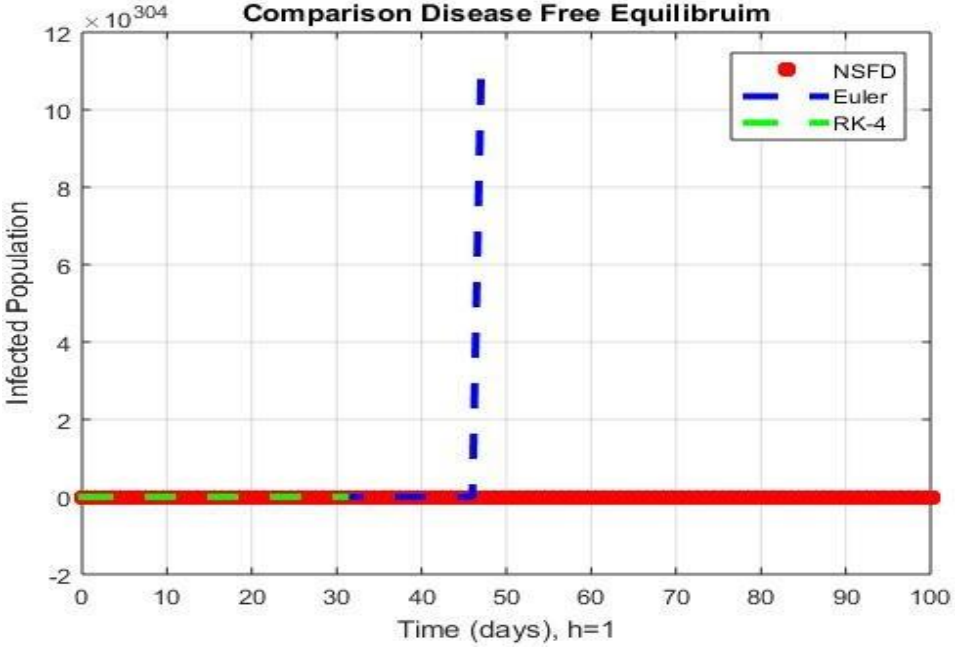

Figure 15. Comparison of Euler, RK-4, and NSFD Scheme at h=0.1

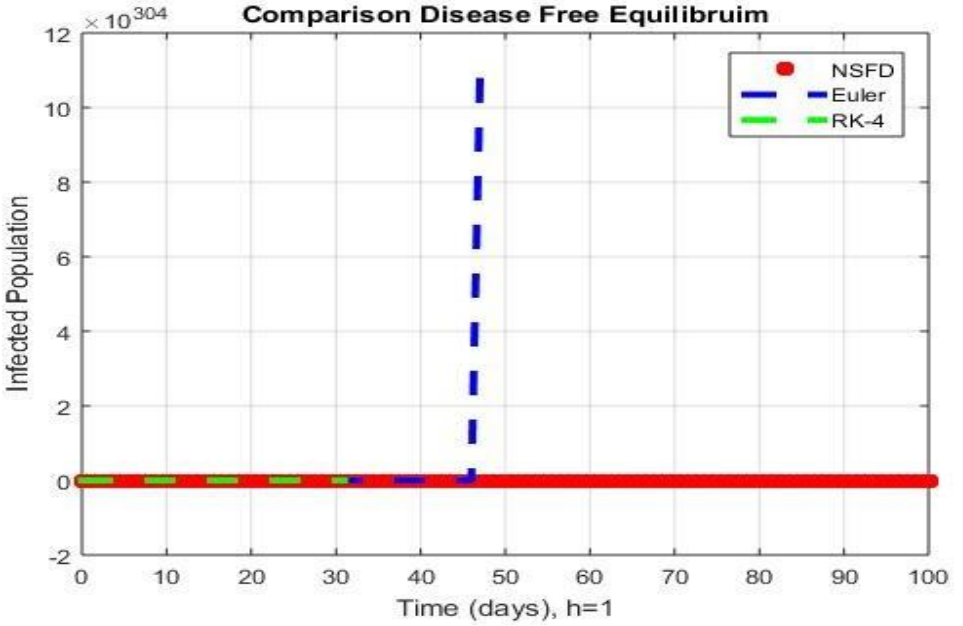

Figure 16. Comparison of Euler, RK-4, and NSFD Scheme at h=1

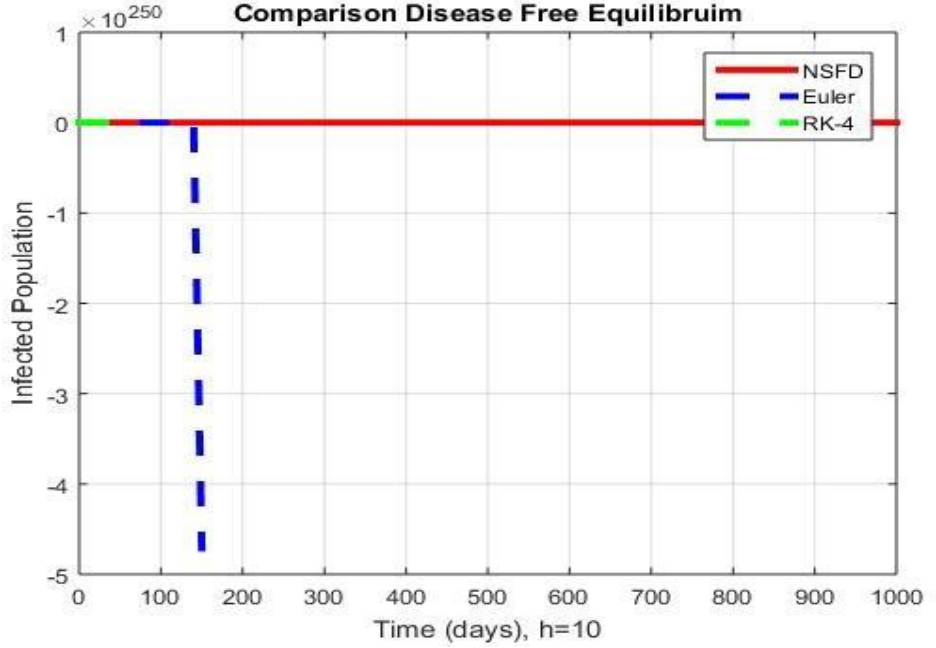

Figure 17. Comparison of Euler, RK-4, and NSFD Scheme at h=10

The behavior of the SEIR model is presented in the above graphs. Figure 2 and Figure 3 show that the Euler technique behaves favorably and converges at small step sizes ($h = 0.01$ and $h = 0.1$). In Figure 4 and Figure 5, the Euler method shows divergence at slightly large step sizes ($h = 1$ and $h = 10$). In Figure 6 and Figure 7, the RK-4 method shows convergence at small step sizes ($h = 0.01$ and $h = 0.1$). The method shows divergence as the step size increases, as shown in Figure 8 and Figure 9, respectively. In Figure 10-13, the NSFD method converges to the same equilibrium points at different step sizes. In Figure 14-17, a comparison of Euler's method, RK-4 method, and NSFD method is depicted. It is clear from the above graphs that all models show similar behaviors at small step sizes and converge to the same equilibrium points. The Euler and RK-4 methods show divergence and negative behavior as step size increases, while the NSFD method converges to the same point. Graphical depiction of behaviors demonstrates that the Euler and RK-4 methods only provide convergence solutions for small step sizes and remain inconclusive for large step sizes. The NSFD scheme, on the other hand, exhibits good behavior and also provides a convergent solution for step sizes that are extremely large.

5. CONCLUSION

The mathematical study of the SEIR model for the spread of COVID-19 was carried out in this research. For this purpose, the reproduction number R_0, sensitivity of R_0, and equilibrium points of the model were determined. It was shown that both equilibrium points have similar stability properties. In order to solve the investigated model, Euler, RK-4, and NSFD algorithms were deployed. Different time step sizes were used for numerical experiments at DFE and EE locations. The collected results were examined and compared. From the said examination, the current study concludes that the suggested method yields findings that converge to true stable states for any time step size. However, the Euler and RK-4 methods do not hold for large time step sizes. Moreover, the NSFD method is bounded, dynamically consistent, and preserves the positivity of the solution which are important requirements when modeling a prevalent disease.

REFERENCES

1. Tyrrell DAJ, Bynoe ML. Cultivation of a novel type of common cold virus in organ culture. *BMJ*. 1965;1(5448):1467–1470. http://dx.doi.org/10.1136/bmj.1.5448.1467

2. World Health Organization. Coronavirus disease (COVID-19). https://www.who.int/health-topics/coronavirus#tab=tab_1

3. Stadler K, Masignani V, Eickmann M, et al. SARS—beginning to understand a new virus. *Nat Rev Microbiol*. 2003;1(3):209–218. https://doi.org/10.1038/nrmicro775

4. Peiris JS, Lai ST, Poon LL, et al. Coronavirus as a possible cause of severe acute respiratory syndrome. *Lancet*. 2003;361(9366):1319–1325. https://doi.org/10.1016/S0140-6736(03)13077-2

5. World Health Organization. Novel coronavirus (2019-nCoV). https://www.who.int/docs/default-source/coronaviruse/situation-reports/20200121-sitrep-1-2019-ncov.pdf . Updated January 21, 2021. Accessed September 18,2021.

6. Abelson R. Brazil reported one of the highest Covid death tolls in the world. *The New York Times*. https://www.nytimes.com/2021/06/20/health/brazil-deaths-covid.html . Updated June 24, 2021. Accessed September 15, 2021.

7. Dhandapani PB, Baleanu D, Thippan J, Sivakumar V. On stiff, fuzzy IRD-14 day average transmission model of COVID-19 pandemic disease. *AIMS Bioeng*. 2020;7(4):208–223.

8. Ullah S, Khan MA. Modeling the impact of non- pharmaceutical interventions on the dynamics of novel coronavirus with optimal control analysis with a case study. *Chaos Solitons Fractal*. 2020;139:e110075. https://doi.org/10.1016/j.chaos.2020.110075

9. Fanelli D, Piazza F. Analysis and forecast of COVID-19 spreading in China, Italy and France. *Chaos Solitons Fractal*. 2020;134:e109761. https://doi.org/10.1016/j.chaos.2020.109761

10. Xiao D, Ruan S. Global analysis of an epidemic model with nonmonotone incidence rate. *Math Biosci*. 2007;208(2):419–429. https://doi.org/10.1016/j.mbs.2006.09.025

11. Lin Q, Zhao S, Gao D, et al. A conceptual model for the coronavirus disease 2019 (COVID-19) outbreak in Wuhan, China with individual reaction and governmental action. *Int J Infect Dis.* 2020:93;211–216. https://doi.org/10.1016/j.ijid.2020.02.058

12. Naveed M, Rafiq M, Raza A, et al. Mathematical analysis of novel

coronavirus (2019-nCov) delay pandemic model. *Comput Mater Continua*. 2020;64(3):1401–1414. https://doi.org/10.32604/cmc.2020.011314

13. Shatanawi W, Raza A, Muhammad Shoaib A, Abodayeh K, Rafiq M, Bibi M. An effective numerical method for the solution of a stochastic coronavirus (2019-nCovid) pandemic model. *Comput Mater Continua.* 2021;66(2):1121–1137.
14. Shahid N, Baleanu D, Ahmed N, et al. Optimality of solution with numerical investigation for coronavirus epidemic model. *Comput Mater Continua.* 2021;67(2):1713–1728. https://doi.org/10.32604/cmc.2021.014191
15. Ahmed N, Baleanu D, Rafiq M, et al., Dynamical behavior and sensitivity analysis of a delayed coronavirus epidemic model. *Comput Mater Continua*. 2020;65(1):225–241. https://doi.org/10.32604/cmc.2020.011534
16. Aba-Oud MA, Ali A, Alrabaiah H, et al. A fractional order mathematical model for COVID-19 dynamics with quarantine, isolation, and environmental viral load. *Adv Differ Equ*. 2021;106:1–19. https://doi.org/10.1186/s13662-021-03265-4
17. Gao W, Veeresha P, Prakasha DG, et al. Novel dynamic structures of 2019-nCOV with nonlocal operator via powerful computational technique. *Biology*. 2020;9(5):e107. https://doi.org/10.3390/biology9050107
18. Khan MA, Atangana A. Modeling the dynamics of novel coronavirus (2019-nCov) with fractional derivative. *Alexandria Eng J*. 2020;59(4):2379–2389. https://doi.org/10.1016/j.aej.2020.02.033
19. Atangana A, Retaraz SIG. A novel Covid-19 model with fractional differential operators with singular and non-singular kernels: Analysis and numerical scheme based on Newton polynomial. *Alexandria Eng J*. 2021;60(4):3781–3806. https://doi.org/10.1016/j.aej.2021.02.016
20. Khan MA, Atangana A, Fatmawati EA. The dynamics of COVID-19 with quarantined and isolation. *Adv Differ Equ*. 2020;2020(1):1–22. https://doi.org/10.1186/s13662-020-02882-9
21. Khan MA, Ullah S, Kumar S. A robust study on 2019-nCOV outbreaks

through non-singular derivative. *Eur Phys J Plus*. 2021;136:e168. https://doi.org/10.1140/epjp/s13360-021-01159-8

22. Rafiq M, Ali J, Riaz MB, et al. Numerical analysis of a bi-modal covid-19 SITR model. *Alexandria Eng J*. 2022;61(1):227–235. https://doi.org/10.1016/j.aej.2021.04.102
23. Mickens RE. Advances in applications of non-standard finite difference schemes. Singapore, World Scientific Publishing Company; 2019.
24. Cresson J, Pierret F. Nonstandard finite difference schemes preserving dynamical properties. *J Comput Appl Math*. 2016;303:15–30. https://doi.org/10.1016/j.cam.2016.02.007
25. Anguelov R, Dumont Y, Lubuma J, Mureithi E. Stability analysis and dynamics preserving nonstandard finite difference schemes for a malaria model. *Math Popul Stud*. 2013;(20):101–122. https://doi.org/10.1080/08898480.2013.777240
26. Riaz S, Rafiq M, Ahmad O. Non standard finite difference method for quadratic riccati differential equation. *Punjab Unive J Math*. 2015;47(2):49–55.
27. Rafiq M, Raza A, Anayat A. Numerical modeling of virus transmission in a computer network. Paper presented at: 14th International Bhurban Conference on Applied Sciences & Technology (IBCAST) 219; January 10–14, 2017; Islamabad, Pakistan. https://doi.org/10.1109/IBCAST.2017.7868087
28. Rafiq M, Ahmad W, Abbas M. et al. A reliable and competitive mathematical analysis of Ebola epidemic model. *Adv Differ Equ*. 2020;2020:e540. https://doi.org/10.1186/s13662-020-02994-2
29. Rafiq M, Ali J, Riaz MB, Jan Awrejcewicz, Numerical analysis of a bi-modal covid-19 SITR model. *Alexandria Eng J*. 2022;61(1):227–235, http://doi/doi.org/10.1016/j.aej.2021.04.102
30. Ahmed N, Tahira S, Rafiq M, et al. Positivity preserving operator splitting nonstandard finite difference methods for SEIR reaction diffusion model. *Open Math*. 2019;17(1):313–330. https://doi.org/10.1515/math-2019-0027
31. Dayan F, Ahmed N, Rafiq M, et al. Construction and numerical analysis of a fuzzy non-standard computational method for the solution of an

SEIQR model of COVID-19 dynamics. *AIMS Math*. 2022;7(5):8449–8470. https://doi.org/10.3934/math.2022471

32. Dayan F, Rafiq M, Ahmed N, et al. Design and numerical analysis of fuzzy nonstandard computational methods for the solution of rumor based fuzzy epidemic model. *Physica A.* 2022;600:e127542. https://doi.org/10.1016/j.physa.2022.127542

33. Dayan F, Ahmed N, Rafiq M, et al. A dynamically consistent approximation for an epidemic model with fuzzy parameters. *Expe Syst Appl*. 2022;210:e118066. https://doi.org/10.1016/j.eswa.2022.118066

34. Dayan F, Rafiq M, Ahmed N, Raza A, Ahmad MO. A dynamical study of a fuzzy epidemic model of Mosquito-Borne Disease. *Comput Biol Med*. 20221;148:e105673. https://doi.org/10.1016/j.compbiomed.2022.105673

35. Dayan F, Baleanu D, Ahmed N, et al., Numerical investigation of malaria disease dynamics in fuzzy environment. *Comput Mater Continua*. 2023;74(2):2345–2361.

36. Raza A, Awrejcewicz J, Rafiq M, Ahmed N, Mohsin M. Stochastic analysis of nonlinear cancer disease model through virotherapy and computational methods. *Mathematics*. 2022;10(3):e368. https://doi.org/10.3390/math10030368

37. Alsallami SA, Raza A, Elmahi M, et al. Computational approximations for Real-World application of epidemic model. *Intell Autom Soft Comput*. 2022;33(3):1923–1939.

38. Chitnis N, Hyman JM, Cushing JM. Determining important parameters in the spread of malaria through the sensitivity analysis of a mathematical model. *Bulletin Math Biol*. 2008;70:1272-1296. https://doi.org/10.1007/s11538-008-9299-0